Current Reviews in Musculoskeletal Medicine (2024) 17:144–156
https://doi.org/10.1007/s12178-024-09892-0

REVIEW

Radiographic and Advanced Imaging Evaluation of Posterior Shoulder Instability

Jennifer A. Knight[1] · **Garret M. Powell**[1] · **Adam C. Johnson**[1]

Accepted: 13 March 2024 / Published online: 12 April 2024

Abstract

Purpose of Review Posterior shoulder instability is an uncommon but important cause of shoulder dysfunction and pain which may occur as the result of seizure, high energy trauma, or repetitive stress related to occupational or sport-specific activities. This current review details the imaging approach to the patient with posterior shoulder instability and describes commonly associated soft tissue and bony pathologies identified by radiographs, CT, and MR imaging.

Recent Findings Advances in MR imaging technology and techniques allow for more accurate evaluation of bone and soft tissue pathology associated with posterior shoulder instability while sparing patients exposure to radiation.

Summary Imaging can contribute significantly to the clinical management of patients with posterior shoulder instability by demonstrating the extent of associated injuries and identifying predisposing anatomic conditions. Radiologic evaluation should be guided by clinical history and physical examination, beginning with radiographs followed by CT and/or MRI for assessment of osseous and soft tissue pathology. Synthesis of a patient's clinical history, physical exam findings, and radiologic examinations should guide clinical management.

Keywords Shoulder · Posterior shoulder instability · MR imaging · Reverse Bankart · POLPSA

Introduction

Posterior shoulder instability is less common than anterior or multidirectional instability, occurring in approximately 10% of all cases of shoulder instability [1]. With improved awareness of the condition, however, it is increasingly recognized as an important cause of shoulder dysfunction and pain especially in young athletic populations [2]. Posterior shoulder instability may occur as the immediate result of a seizure or high-energy trauma, or may evolve gradually due to repetitive stress related to occupational or sport-specific activities. Posterior shoulder instability may be challenging to diagnose as patients commonly present with weakness and pain rather than frank shoulder instability [3]. While posterior shoulder instability remains a clinical diagnosis, radiologic evaluation with radiographs and cross-sectional imaging can guide clinical management by identifying anatomic conditions that predispose to shoulder instability and characterizing associated injuries. This review discusses the imaging approach to posterior shoulder instability and describes commonly associated soft tissue and osseous pathology.

Relevant Imaging Anatomy

The glenohumeral joint is a ball-and-socket articulation between the scapular glenoid and proximal humerus. The small shallow articular surface of the glenoid and large articular surface of the spherical humeral head allow for a large range of motion but also predispose the joint to instability [4]. The stability of the glenohumeral joint is therefore reliant on dynamic and static stabilizers to preserve its articulation [5]. Degeneration, injury, or congenital variation of one or multiple of these components may result in shoulder dislocation or instability.

✉ Jennifer A. Knight
knight.jennifer@mayo.edu

Garret M. Powell
powell.garret@mayo.edu

Adam C. Johnson
johnson.adam@mayo.edu

[1] Department of Radiology, Mayo Clinic, Charlton Building North, 1st Floor, 200 First Street SW, Rochester, MN 55905, USA

The glenoid labrum, glenohumeral ligaments, and joint capsule act as the primary static soft tissue stabilizers of the glenohumeral joint [5]. The glenoid labrum is a fibrocartilage structure extending circumferentially along the glenoid rim which increases the concavity and depth of the glenoid, improves humeral head contact, and contributes to a suction seal effect [6, 7]. The labrum is best demonstrated on orthogonal axial and coronal oblique magnetic resonance imaging (MRI), typically appearing hypointense on all MRI sequences and rounded or triangular in morphology (Fig. 1). While labral anatomic variants are commonly seen superiorly and anterosuperiorly, including the sublabral foramen and sublabral recess, the normal posterior labrum is securely anchored to the posterior glenoid rim [6].

The osseous rim of the glenoid and fibrocartilaginous labrum serves as attachment sites for the superior, middle, and inferior glenohumeral ligaments, discrete fibrous components of the joint capsule, which passively stabilize the joint at the extremes of motion [8]. On MRI, the glenohumeral ligaments appear as linear hypointense structures extending from the anterior and inferior glenoid to the humerus, best seen when the joint is distended by intraarticular contrast or an effusion (Fig. 1). The inferior glenohumeral ligament is formed by anterior and posterior bands bordering the axillary pouch, which span the axillary recess. The posterior band of the inferior glenohumeral ligament (PIGHL), in conjunction with joint capsule and posterior labrum, stabilizes the humeral head in forward flexion and internal rotation [9].

The rotator cuff, periscapular musculature, and long head of the biceps tendon act as the primary dynamic stabilizers of the glenohumeral joint [5, 10]. These structures contribute to joint stability by dynamically compressing the humeral head into the glenoid throughout the shoulder's range of motion, a phenomenon known as concavity compression [10]. The subscapularis, in particular, acts as an important dynamic stabilizer preventing posterior translation of the humeral head [11].

Imaging Techniques

Radiographs

Initial radiologic evaluation of the patient with posterior shoulder instability begins with radiographs. Radiographs provide an overview of glenohumeral alignment and bony anatomy, as well as an initial assessment for fractures, osteocartilaginous bodies, and soft tissue calcifications. A standard shoulder series begins with anteroposterior (AP) radiographs with the arm in external and internal rotation, as well as a neutrally rotated true AP (Grashey) radiographs providing a tangential view of the glenohumeral joint space. Orthogonal axillary views are obtained with the shoulder in 90° of abduction. In particular, the axillary view is useful to assess the anteroposterior glenohumeral alignment and to evaluate for reverse Hill-Sachs lesions, fractures of the glenoid rim or bony avulsions in the setting of posterior shoulder instability. In patients who are unable to fully abduct their shoulder, a scapular Y (Neer) view obtained longitudinally down the axis of the scapula with the patient upright or prone can be considered [12]. If clinically warranted, additional specialized views, including the Stryker notch and West-point axillary views, may be considered for more sensitive assessment of humeral and glenoid bone loss [13]. Notably, in many cases of posterior shoulder instability, radiographs may be negative.

MR Imaging

MRI is the gold standard for assessing soft tissue static and dynamic glenohumeral stabilizers. MRI evaluation of the

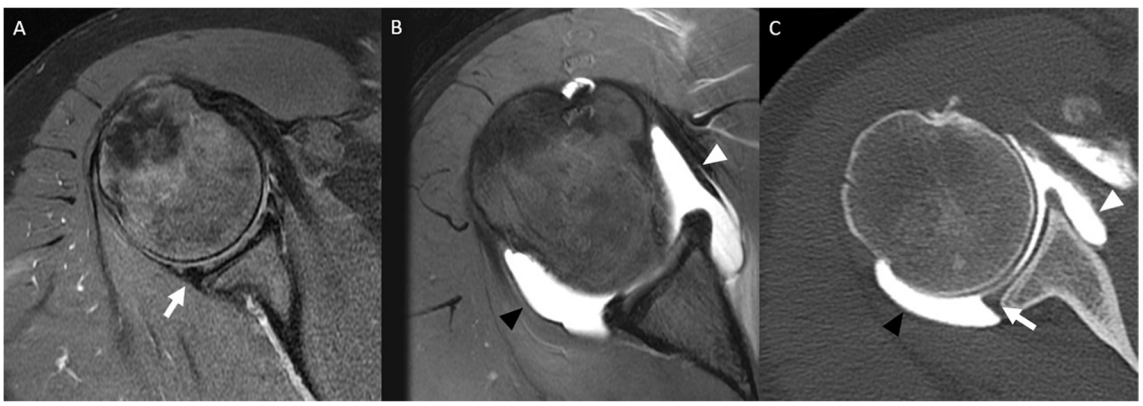

Fig. 1 Axial T2FS MR image (**A**) shows normal dark triangular appearance of intact posterior labrum (white arrow). Axial T1FS MR arthrogram image (**B**) shows the anterior (white arrowhead) and posterior (black arrowhead) bands of the inferior glenohumeral ligament. Axial CT arthrogram image (**C**) shows intact AIGHL (white arrowhead), PIGHL (black arrowhead), and posterior labrum (white arrow)

shoulder can be performed at either 1.5 T or 3 T; however, 3 T is preferred due to its higher spatial resolution. The patient is typically positioned with the arm in partial external rotation with the shoulder as close to the magnet's isocenter as possible [14]. A dedicated shoulder phased array surface coil is used to maximize the signal-to-noise ratio. When a shoulder coil cannot be used, a large multichannel phased array flexible coil can be wrapped around the shoulder. At our institution, MRI evaluation of the shoulder includes T1-weighted or proton density and fat saturated fluid sensitive high resolution (384 × 280 matrix, 4-mm slice thickness) intermediate echo time fast spin echo (FSE) sequences obtained in axial, oblique sagittal, and oblique coronal planes. At least one T1-weighted plane (typically sagittal) is obtained for optimal assessment of bone marrow signal and rotator cuff musculature quality.

Many authors advocate for MR arthrography (MRA) over conventional MRI in patients with shoulder instability [8, 15, 16]. In a recent study, the sensitivity and specificity of MRA for identification of posterior labral tears were 84% and 88% respectively [17••]. At our institution, MRA is performed using 10–12 cc of a 1:200 dilution of gadolinium contrast instilled into the glenohumeral joint space under fluoroscopic guidance prior to image acquisition. High-resolution (384 × 280, 4-mm slice thickness) axial and coronal FSE fat-saturated T1-weighted images; sagittal FSE T1-weighted images; and axial, coronal, and sagittal FSE fat saturated T2-weighted images are acquired. MRA results in capsular distention, which delineates the labrum and capsuloligamentous structures and improves detection of labral abnormalities when compared with conventional MRI [18, 19].

MR imaging at 3 T has significantly improved signal, spatial resolution, and acquisition speed compared to 1.5 T and has raised question of the utility of MRA. While several meta-analyses have shown increased sensitivity and specificity of MRA for the identification of glenoid labral tears when compared to conventional MRI, these differences were relatively minor [20•, 21]. At our institution, the use of MRA is still favored in young patients in whom a reparable labral tear is suspected or when evaluating a previously repaired labrum.

CT Imaging

Computed tomography (CT) evaluation is the gold standard for assessing the bony anatomy of the shoulder [22]. CT scans have high spatial resolution which optimizes the evaluation of bone cortex and morphology. When acquired with isotropic thin collimation (0.600 mm), 3D volume-rendered reconstructions can be created to further assess osseous abnormalities; for example, the scapula can be isolated and reconstructed in 3D to assess glenoid morphology and bone loss with digital removal of the adjacent bones and soft tissues to optimize assessment.

Historically, CT arthrography is utilized when there are absolute or relative contraindications to MR imaging such as incompatible implanted devices, retained ferromagnetic material, regional hardware, and patients with severe claustrophobia [23]. However, advances in multidetector CT resulting in higher spatial and contrast resolution have sparked new interest in CT arthrography (Fig. 1). In the context of shoulder instability, multidetector CT arthrography and MR arthrography have similar accuracy for detecting cartilage and labroligamentous abnormalities [23, 24]. Additionally, due to the higher spatial resolution of CT and CT arthrography, the characterization of osseous abnormalities and detection of other pathologies (e.g., Bennett lesion) may be greater compared to MR arthrography [23].

Bone Pathology

Glenoid Bone Loss

In patients with posterior shoulder instability, decreased functional glenoid width due to bone loss is commonly identified [25, 26]. Posterior glenoid bone loss can occur as the result of an acute posterior dislocation or chronic attritional bone loss which may worsen with repeated instability events [27•]. Decreased glenoid width is associated with poor outcomes and recurrent instability following posterior labroligamentous repair; therefore, preoperative identification and accurate characterization of the glenoid are important in guiding management [28, 29].

Glenoid bone loss is accurately determined using CT and various linear and surface area methods can be used. In a commonly used linear diameter-based method, the articular surface of the glenoid is framed with a best fit circle in the sagittal plane, and the glenoid defect is measured from the deepest margin to the best fit circle [30]. The defect distance is then divided by the diameter of the best fit circle to calculate the percent bone loss of the glenoid defect (Fig. 2).

Alternatively, a surface area-based method may be utilized, in which a best fit circle is similarly aligned to the glenoid and the defect is freehand traced using specialized software to obtain the respective surface areas. Then, the surface area of the glenoid defect is divided by that of the best fit circle to determine the percentage of glenoid surface area loss [28]. Although some authors have found more accuracy and reliability with surface area techniques compared to linear techniques [31, 32], they require specialized software and additional operator time, which has limited their widespread use.

MRI has been increasingly utilized to quantitatively assess glenoid bone loss. While some authors have shown

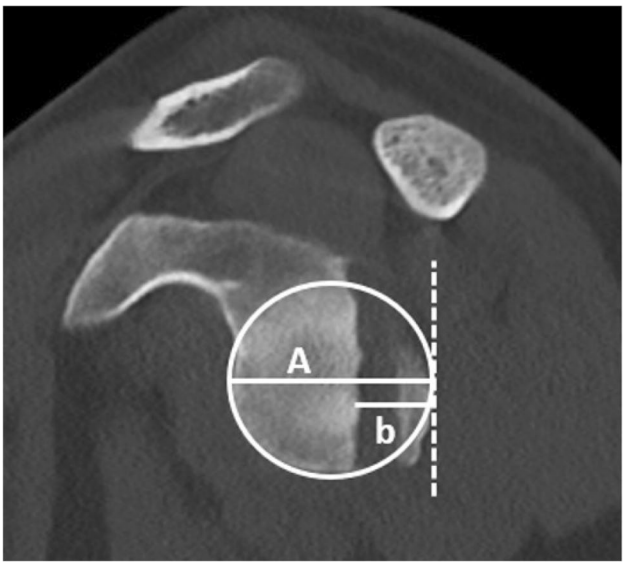

Fig. 2 Sagittal CT image demonstrates measuring the extent of glenoid bone loss in the setting of a reverse bony Bankart using the best-fit-circle method, which superimposes a circle over the glenoid articular surface. The defect size (b) divided by the glenoid diameter (A) equals the percentage of glenoid bone loss

similar accuracy of determining glenoid bone loss with MRI and 2D CT [30, 33], others have found decreased accuracy and worse interobserver reliability of MR compared to 3D CT [22, 34]. Recent investigations assessing glenoid morphology with MR have included a zero-echo time (ZTE) sequence which utilizes a near-zero echo time to assess short-T2 tissues (e.g., bone) and ultimately produces images similar to CT [35–37]. While this technique has increasingly been used in musculoskeletal imaging, the spatial resolution remains inferior to CT and image post-processing requires additional time and specialized training, constraints which may limit its widespread use [37].

Reverse Bony Bankart

A well-known cause of posterior glenoid bone loss is the reverse bony Bankart lesion which is a posteroinferior glenoid fracture with associated disruption of the posterior labroligamentous complex. Following an acute posterior shoulder dislocation, the reverse bony Bankart lesion can be seen in up to 86% of patients [38]. Additionally, the reverse bony Bankart lesion predisposes to recurrent instability [1]. The associated fracture can vary in size and the degree of fragmentation. The axial and sagittal oblique planes on cross-sectional imaging are best for evaluating a reverse bony Bankart lesion (Fig. 3). Notably, MR imaging is less accurate for the detection of small bony Bankart lesions compared to CT, particularly if fat suppressed sequences are utilized [39].

Glenoid Dysplasia

Glenoid dysplasia is a developmental osseous deficiency of the posterior glenoid which can be abnormally rounded or have an increased posterior slope (Fig. 4). This altered morphology decreases the effective glenoid concavity and may predispose to posterior instability [40, 41]. An abnormality in ossification of the inferior glenoid pre-cartilage is thought to result in glenoid dysplasia [42]. The dominant osseous sequalae of glenoid dysplasia are the "lazy J" morphology with rounding of the posteroinferior glenoid and the "delta" morphology with a more abrupt angular deficiency of the posteroinferior glenoid [41]. Various grades can be applied to glenoid dysplasia based on the glenoid morphology, degree of osseous deficiency, and severity of the posterior slope as described by Harper et al. [40]. Glenoid dysplasia is associated with compensatory labral and articular cartilage overgrowth overlying the osseous deficiency, which allows for differentiating developmental dysplasia from post-traumatic and attritional bone loss due to recurrent posterior instability [43].

Glenoid Retroversion

Glenoid version refers to the angulation of the glenoid articular surface relative to the axis of the scapular body. Normal glenoid version is essentially 0°, often with slight anteversion or retroversion varying less than 10° in either direction [44]. Increased glenoid retroversion may predispose patients to posterior shoulder instability, with higher degrees of retroversion conveying increased risk [1, 45–47]. In a prospective study of 714 military cadets, Owens et al. found glenoid retroversion to be an independent risk factor for posterior shoulder instability and that for every 1° of increased glenoid retroversion, the risk of posterior shoulder instability increased by 17% [1].

The degree of glenoid version can be measured utilizing the method outlined by Friedman et al. [48]. In this method, axial MRI or CT images are used to establish the scapular axis, defined by a line drawn from medial border of the scapula to the midpoint of the glenoid articular surface. Glenoid version is then measured as the angle between a line drawn perpendicular to the scapular axis and a line drawn tangent to the face of the glenoid (Fig. 5).

Reverse Hill-Sachs

The reverse Hill-Sachs lesion is a fracture of the anteromedial humeral head due to impaction of the humeral head onto the posterior glenoid rim during posterior shoulder dislocation [49]. Reverse Hill-Sachs lesions present with loss of the normal convexity of the anteromedial humeral head, best appreciated on AP and axillary radiographs or axial

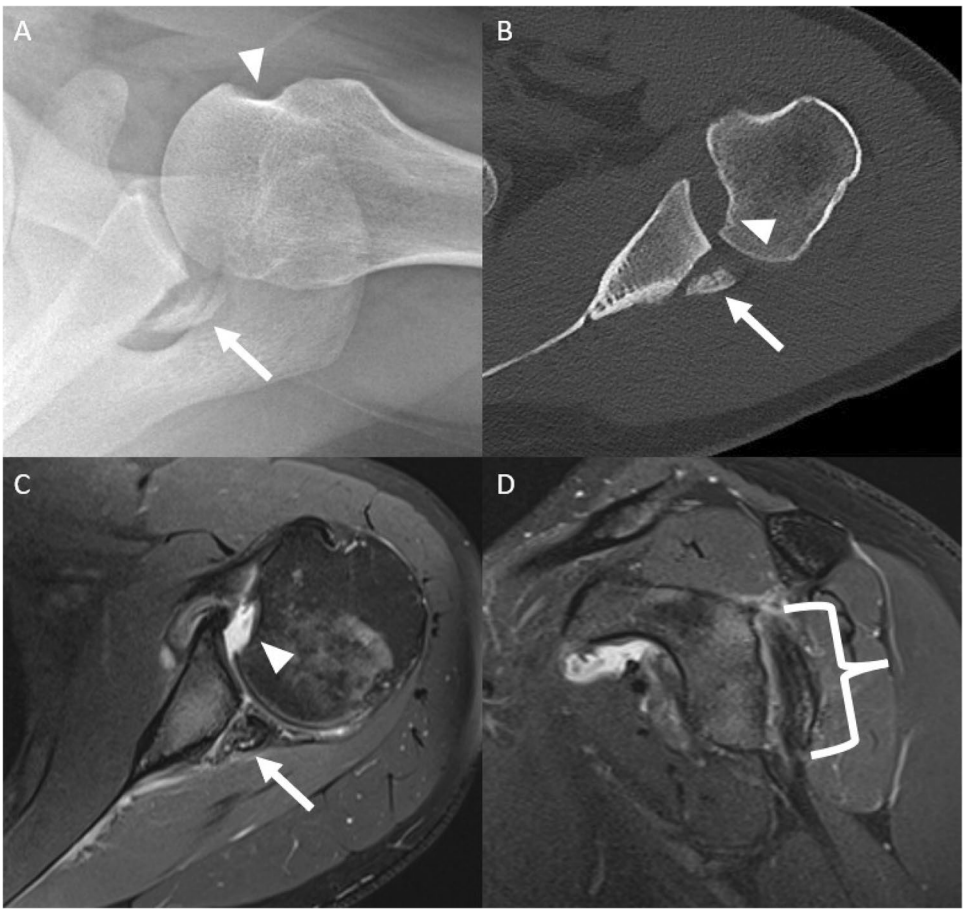

Fig. 3 Axillary radiograph (**A**), axial CT (**B**), and axial T2 fat-saturated MR (**C**) images demonstrate a reverse bony Bankart lesion (arrow) and a reverse Hill-Sachs impaction fracture (arrowhead). Sagittal T2 fat-saturated image (**D**) demonstrates the extent of the reverse bony Bankart lesion (bracket). Additionally, there is posterior subluxation of the humeral head relative to the glenoid (**B** and **C**)

cross-sectional imaging (Fig. 3). These lesions can increase the risk of recurrent posterior instability and dislocation, particularly if greater than 30% of the articular surface is involved or if there are concurrent injuries to posterior soft tissue static stabilizers [50].

A standardized method for measuring humeral head bone loss on CT was proposed by Moroder et al. In this technique, axial images best demonstrating the reverse Hill-Sachs defect are utilized and a best fit circle is aligned with the intact margins of the humeral head articular surface. The defect extent (alpha angle) is measured by drawing radial lines from the margins of the defect to the center of the best fit circle. The angle between these lines represents the superficial extent of the defect in terms of alpha degrees [51, 52]. The depth of the defect is measured as the distance from the margin of the best fit circle to the base of the defect, which is then divided by the diameter of the circle to obtain the relative percentage bone loss [51, 52]. Moroder

Fig. 4 Axillary radiograph (**A**), axial CT (**B**), and axial T2 fat-saturated MR (**C**) images demonstrate glenoid dysplasia with associated overgrowth of the posterior glenoid cartilage best seen on MR (arrow)

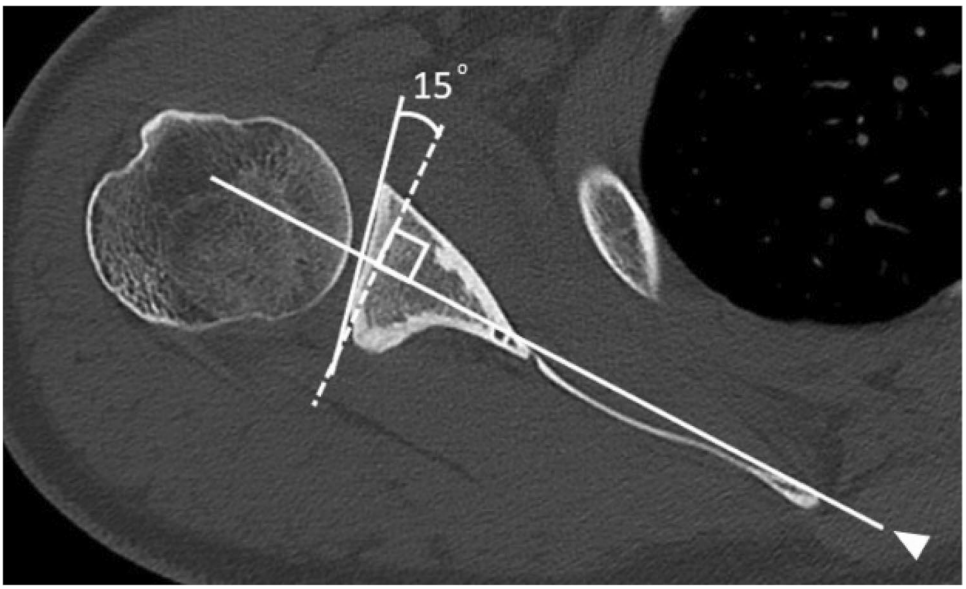

Fig. 5 Axial CT image demonstrates glenoid retroversion measuring 15° in the setting of glenoid dysplasia. By creating a line through the scapular axis (arrowhead), glenoid version can be measured as the angle between the glenoid articular surface and a line perpendicular to the scapular axis

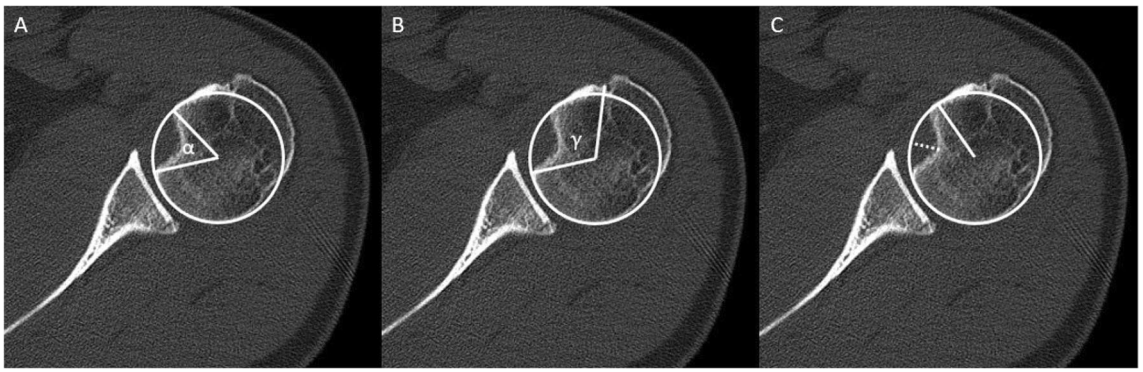

Fig. 6 Axial CT images utilizing best-fit-circle method to quantify alpha angle (**A**), gamma angle (**B**), and defect depth measurement measured as a dotted line (**C**)

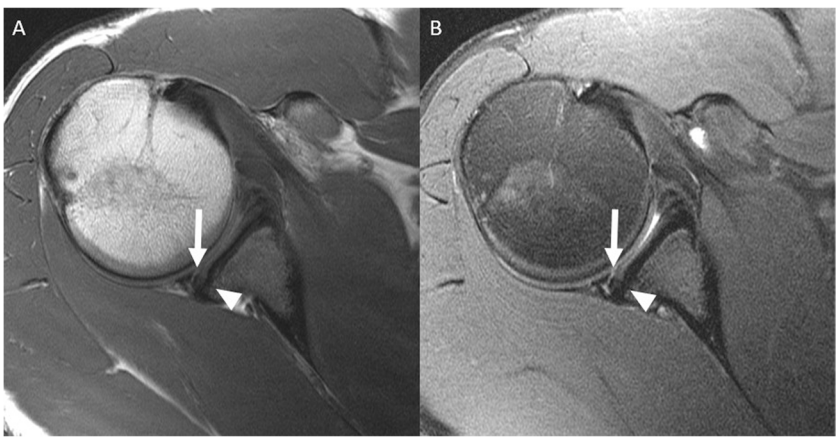

Fig. 7 Axial PD (**A**) and T2 fat-saturated (**B**) MR images demonstrate a reverse Bankart lesion (arrow) in the setting of posterior glenoid dysplasia (arrowhead)

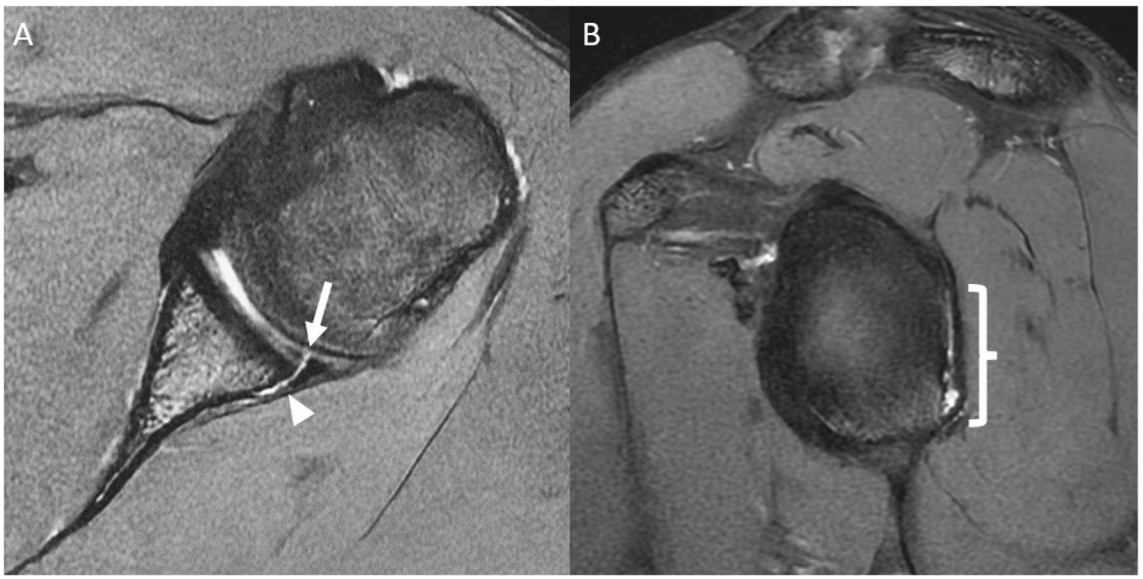

Fig. 8 Axial (**A**) and sagittal (**B**) T2 fat-saturated MR images demonstrate a tear of the posteroinferior chondrolabral junction (arrow) with associated stripping of the posterior glenoid periosteum (arrowhead) consistent with a posterior labrocapsular periosteal sleeve avulsion lesion. The extent of periosteal stripping (bracket) is well seen in the sagittal plane

et al. also described the "gamma angle" as a predictor of the risk of re-engagement of a reverse Hill-Sachs lesion. The gamma angle is measured from the center of the best fit circle on axial images to the bicipital groove and posterior margin of the defect (Fig. 6). A gamma angle > 90° was found by Moroder et al. to convey an increased risk of re-engagement of the humeral head defect with the posterior glenoid rim [51].

Labroligamentous Pathology

Reverse Bankart

A reverse Bankart lesion is a tear of the posteroinferior labrum and adjacent posterior scapular periosteum with resulting detachment of the labrum from the glenoid [49]. These lesions are primarily seen in the setting of posterior shoulder dislocations, occurring due to impaction of the humeral head on the labrum or excessive tension on the labrum from the PIGHL with the humeral head abducted and internally rotated [6]. The resulting disruption of the posterior labroligamentous complex destabilizes the PIGHL resulting in posterior decentering of the humeral head [53]. On conventional MRI or MRA, a reverse Bankart lesion is identified by fluid signal intensity or contrast extending through the substance of the posterior labrum or chondrolabral junction with disruption of the scapular periosteum and detachment of the labrum from the glenoid [53] (Fig. 7).

POLPSA

Posterior labrocapsular periosteal sleeve avulsion (POLPSA) is a variant of the reverse Bankart lesion and a counterpart to the ALPSA lesion associated with anterior shoulder instability [6]. With POLPSA, the posteroinferior labroligamentous complex is separated from the posterior glenoid; however,

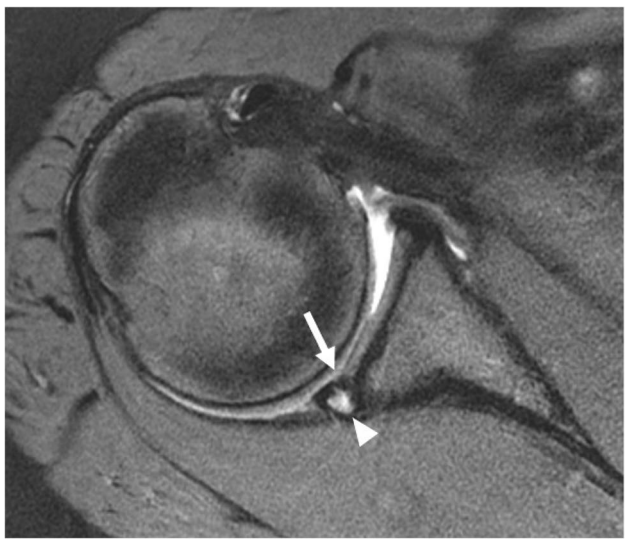

Fig. 9 Axial T2 fat-saturated MR image demonstrates posterior decentering of the humeral head relative to the glenoid, subtle incomplete tear ("marginal crack") of the posterior chondrolabral junction (arrow), and a cyst-like fluid collection between the glenoid and deep labrum (arrowhead) consistent with Kim's lesion

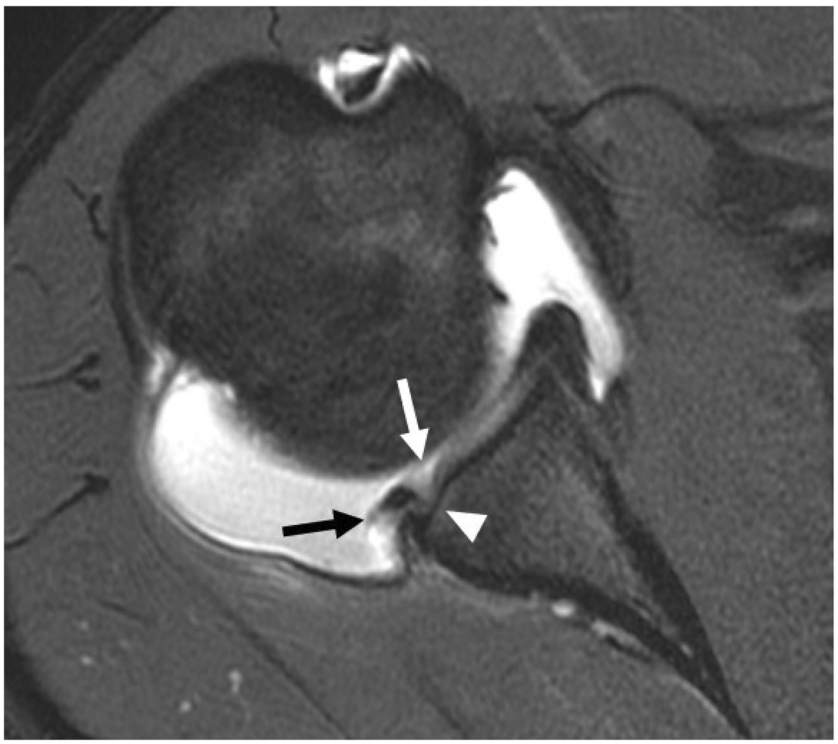

Fig. 10 Axial T2 fat-saturated MR arthrogram image demonstrates a tear of the posteroinferior glenoid labrum (black arrow) with an associated articular cartilage defect (white arrow) consistent with posterior glenolabral articular disruption. Additionally, there is attritional bone loss of the posteroinferior glenoid (arrowhead)

Fig. 11 Axial T2 fat-saturated MR image demonstrates a full-thickness tear of the posterior band of the inferior glenohumeral ligament from its humeral attachment (arrow) with associated extracapsular joint fluid along the PIGHL (arrowhead) consistent with a posterior humeral avulsion of the inferior glenohumeral ligament

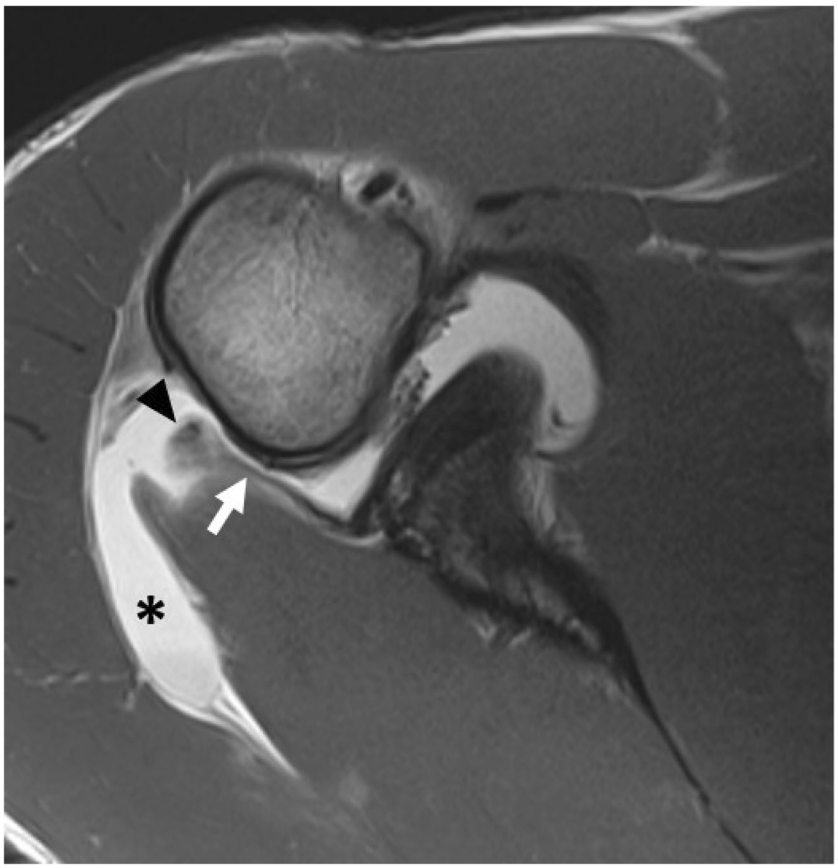

Fig. 12 Axial PD MR image demonstrates a functional full-thickness tear of the posterior band of the inferior glenohumeral ligament, which is lax or "wavy" (arrow), associated avulsive fragment (arrowhead) from the humerus, and extracapsular joint fluid (asterisk) consistent with a bony posterior humeral avulsion of the inferior glenohumeral ligament

unlike reverse Bankart injuries, the associated scapular periosteum remains attached to the labral tissue and is stripped posteromedially, forming a redundant recess or "periosteal sleeve" in communication with the joint space [54, 55]. On conventional MRI or MRA, a POLPSA lesion may appear as a deformed labroligamentous complex displaced medially relative to the glenoid with an intact but stripped periosteum and patulous posterior joint capsule (Fig. 8). In the setting of a chronic POLPSA lesion, organized scarring and fibrous tissue may form in the periosteal sleeve, thereby limiting detection of the lesion by conventional MRI or MRA [54].

Kim's Lesion

A unique pattern of labral injury associated with posterior shoulder instability is Kim's lesion. Kim's lesion is defined as an incomplete separation of the posteroinferior labrum from the glenoid accompanied by a superficial tear at the chondrolabral junction, described as a "marginal crack" [6, 56] (Fig. 9). The injury is thought to occur due to repetitive microtrauma from posteriorly directed force during overhead or forward pressing activities [46]. MR arthrography findings of Kim's lesion include incomplete chondrolabral separation of the posterior labrum and decreased labral height [6, 56]. In many cases, however, the lesion may be occult on MRI and is only identified upon probing the labrum during arthroscopy [56]. It is important to recognize this challenging entity as it can lead to repeated episodes of posterior instability if not identified.

Posterior Glenolabral Articular Disruption

The posterior glenolabral articular disruption (posterior GLAD) lesion is the counterpart to the GLAD lesions seen in anterior shoulder instability. Posterior GLAD lesions present on MR imaging as subtle nondisplaced or minimally displaced tears at the posteroinferior margin of the glenoid labrum with an associated injury of the adjacent articular cartilage [49] (Fig. 10). The degree of cartilage damage associated with a GLAD lesion may range from surface fibrillation to deep chondral loss or chondral detachment resulting in the formation of an intraarticular loose body.

Posterior Humeral Avulsion of the Inferior Glenohumeral Ligament

Posterior humeral avulsion of the glenohumeral ligament (PHAGL) is a rare injury associated with posterior shoulder instability that may occur as the result of posterior shoulder

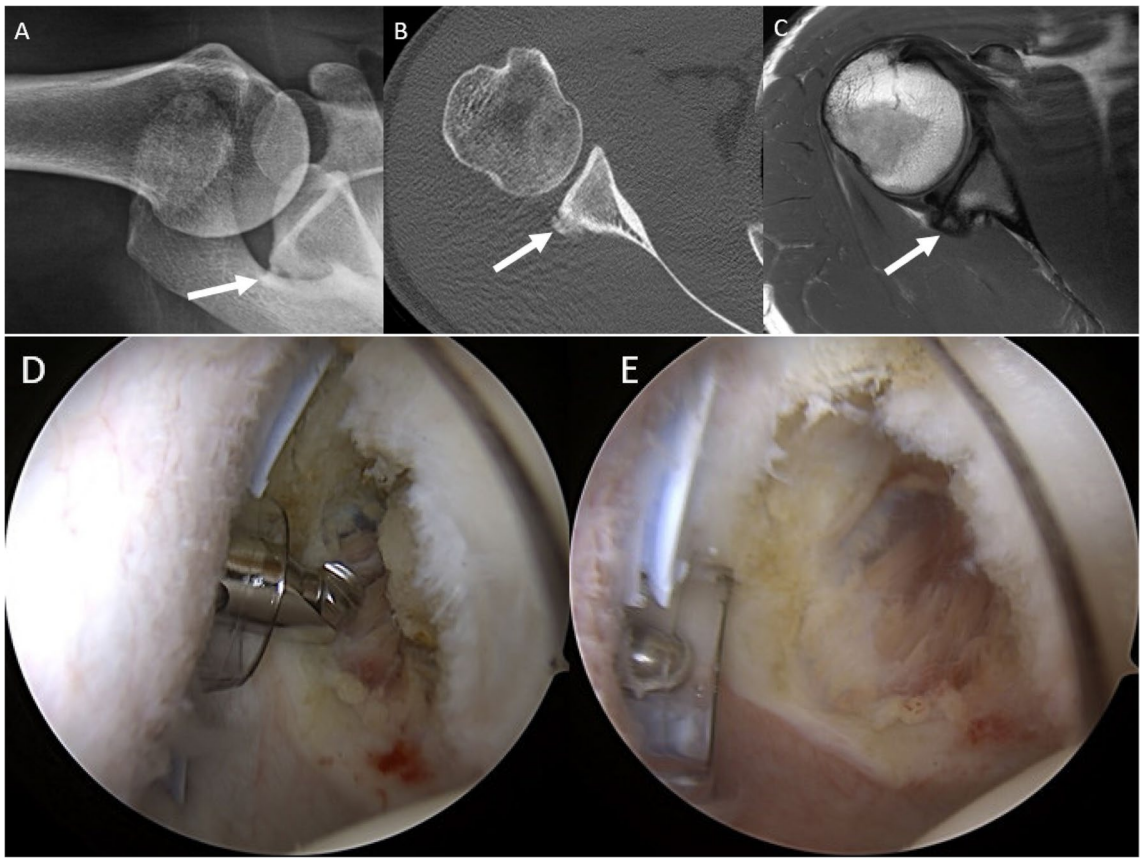

Fig. 13 Axillary view radiograph (**A**), axial CT (**B**), and axial PD MR images (**C**) demonstrate a small curvilinear focus of ossification along the posterior glenoid consistent with a Bennett lesion (arrow). Arthroscopic images of the same patient before (**D**) and after (**E**) debridement of the lesion

dislocation or repetitive microtrauma [57, 58]. PHAGL lesions are identified on MR imaging or CT arthrography as a complete avulsion of the PIGHL from its humeral attachment, best seen on coronal oblique or axial T2 fat saturated sequences [57, 59]. The PIGHL attaches at the posterior margin of the greater tuberosity and deep to the infraspinatus. Disruption is identified as a focal fluid filled defect at this site with or without a lax or "wavy" appearance of the PIGHL and surrounding extracapsular soft tissue edema (Fig. 11). Chronic PHAGL lesions can be occult on imaging as scar tissue may form at the site of injury, mimicking the appearance of an intact ligament [60]. Isolated PHAGL injuries are rare and most injuries to the PIGHL are associated with concurrent posterior or inferior labral injuries, bony Bankart, Hill-Sachs lesions, and rotator cuff tears [61•].

In rare instances, a PHAGL lesion is associated with a concurrent reverse Bankart or Bankart variant posterior labral tear with resulting disruptions of both the humeral and glenoid attachments of the PIGHL, referred to as a "floating" PIGHL [62]. The glenoid sided counterpart to the PHAGL lesion is the reverse glenoid avulsion of the glenohumeral ligament (reverse GAGL). This lesion appears as a tear of the posterior capsule/PIGHL from its glenoid attachment, often with concurrent capsular stripping from the posterior labrum [49].

In a small proportion of patients, PHAGL or reverse GAGL lesions may be associated with an avulsive bony fragment from their attachments on the humerus or glenoid rim, respectively referred to as bony PHAGL (Fig. 12) or bony reverse GAGL lesions [49]. These lesions are best identified on plain radiographs or CT, presenting as small bony fragments adjacent to the posteromedial cortex of the humeral neck or posterior rim of the glenoid which mimic the appearance of a calcified intra-articular loose body or reverse bony Bankart lesion.

Bennett Lesion

Bennett lesions are curvilinear extraarticular foci of mineral production that extend along the posterior inferior rim of the glenoid, closely approximating the attachment of the PIGHL [63]. Seen almost exclusively in over-head throwers, the

Bennett lesion is considered the sequelae of a chronic stress-related traction injury on the PIGHL during the deceleration phase of throwing or impingement of the humeral head on the posterior glenoid during the cocking phase [64, 65]. The Bennett lesion presents as a curvilinear calcification/ossification along the posteroinferior margin of the glenoid, best seen on axillary radiographs or axial CT (Fig. 13) and may occur in conjunction with a tear of the posterior labrum in symptomatic shoulders [66].

Conclusion

While posterior shoulder instability is ultimately a clinical diagnosis, imaging can significantly contribute to clinical management by demonstrating associated soft tissue and bony injuries and identifying anatomic conditions that may predispose to instability. Imaging evaluation should begin with radiographs, which are utilized to identify joint malalignment, fractures, or soft tissue calcifications. Subsequent CT or MRI allows for more sensitive identification and quantification of osseous pathology and enables detailed evaluation of the labroligamentous structures. The patient's clinical history, physical exam findings, and radiologic examinations should be synthesized to guide clinical management.

Author Contributions JK wrote the main manuscript text. AJ and GP prepared the figures. All authors reviewed the manuscript.

Data Availability No datasets were generated or analysed during the current study.

Compliance with Ethical Standards

Competing Interests The authors declare no competing interests.

Human and Animal Rights and Informed Consent This article does not contain any studies with human or animal subjects performed by any of the authors.

References

Papers of particular interest, published recently, have been highlighted as:
- • Of importance
- •• Of major importance

1. Owens BD, Campbell SE, Cameron KL. Risk factors for posterior shoulder instability in young athletes. Am J Sports Med. 2013;41:2645–9. https://doi.org/10.1177/0363546513501508.
2. Lanzi JT, Chandler PJ, Cameron KL, et al. Epidemiology of posterior glenohumeral instability in a young athletic population. Am J Sports Med. 2017;45:3315–21. https://doi.org/10.1177/0363546517725067.
3. Lee J, Woodmass JM, Bernard CD, et al. Nonoperative management of posterior shoulder instability: what are the long-term clinical outcomes. Clin J Sport Med. 2022;32(2):e116–20. https://doi.org/10.1097/JSM.0000000000000907.
4. Pastor MF, Smith T, Struck M, Wellmann M. Stability versus mobility of the shoulder. Biomechanical aspects in athletes Orthopade. 2014;43(3):209–14. https://doi.org/10.1007/s00132-013-2142-9.
5. Lugo R, Kung P, Ma CB. Shoulder biomechanics. Eur J Radiol. 2008;68(1):16–24. https://doi.org/10.1016/j.ejrad.2008.02.051.
6. De Coninck T, Ngai SS, Tafur M, Chung CB. Imaging the glenoid labrum and labral tears. Radiographics. 2016;36(6):1628–47. https://doi.org/10.1148/rg.2016160020. (PMID: 27726737).
7. Ishikawa H, Henninger HB, Kawakami J, et al. A stabilizing role of the glenoid labrum: the suction cup effect. J Shoulder Elbow Surg. 2023;32(5):1095–104. https://doi.org/10.1016/j.jse.2022.12.002.
8. Roy EA, Cheyne I, Andrews GT, Forster BB. Beyond the cuff: MR imaging of labroligamentous injuries in the athletic shoulder. Radiology. 2016;278(2):316–32. https://doi.org/10.1148/radiol.2015150364.
9. Provencher MT, LeClere LE, King S, et al. Posterior instability of the shoulder: diagnosis and management. Am J Sports Med. 2011;39(4):874–86. https://doi.org/10.1177/0363546510384232.
10. Lippitt S, Matsen F. Mechanisms of glenohumeral joint stability. Clin Orthop Relat Res. 1993;291:20–8.
11. Matsen FA, Chebli C, Lippitt S. Principles for the evaluation and management of shoulder instability. J Bone Joint Surg Am. 2006;88(3):648–59.
12. Cruz SA, Castillow H, Chintapalli RT, et al. The clinical utility of additional axillary and Velpeau radiographs in the evaluation of suspected shoulder trauma. J Orthop Trauma. 2020;34(8):261–5. https://doi.org/10.1097/BOT.0000000000001760.
13. Sanders TG, Jersey SL. Conventional radiography of the shoulder. Semin Roentgenol. 2005;40(3):207–22. https://doi.org/10.1053/j.ro.2005.01.012.
14. Alaia EF, Subhas N. Shoulder MR imaging and MR arthrography techniques: new advances. Magn Reason Imaging Clin N Am. 2020;28(2):153–63. https://doi.org/10.1016/j.mric.2019.12.001.
15. Woertler K, Waldt S. MR imaging in sports-related glenohumeral instability. Eur Radiol. 2006;16:2622–36. https://doi.org/10.1007/s00330-006-0258-6.
16. Waltz DM, Burge AJ, Steinbach L. Imaging of shoulder instability. Semin Musculoskelet Radiol. 2015;19(3):254–68. https://doi.org/10.1055/s-0035-1549319.
17. •• Rixey A, Rhodes N, Murthy N, et al. Accuracy of MR arthrography in the detection of posterior glenoid labral injuries of the shoulder. Skeletal Radiol. 2023;52(2):175–81. https://doi.org/10.1007/s00256-022-04165-8. **This study demonstrates the high sensitivity and specificity of MR arthrography for detection of posterior glenoid labral injuries.**
18. Flannigan B, Kursunoglu-Brahme S, Snyder S, et al. MR arthrography of the shoulder: comparison with conventional MR imaging. AJR Am J Roentgenol. 1990;155(4):829–32. https://doi.org/10.2214/ajr.155.4.2119117.
19. Major NM, Browne J, Domzalski T, et al. Evaluation of the glenoid labrum with 3-T MRI: is intraarticular contrast necessary? AJR Am J Roentgenol. 2011;196(5):1139–44. https://doi.org/10.2214/AJR.08.1734.
20. • Smith TO, Drew BT, Toms AP. A meta-analysis of the diagnostic test accuracy of MRA and MRI for the detection of glenoid labral injury. Arch Orthop Trauma Surg. 2021;132(7):905–19.

https://doi.org/10.1007/s00402-012-1493-8. **Recent meta-analysis showing slightly increased sensitivity and specificity of MRA over conventional MRI for detection of glenohumeral labral injuries.**

21. Ajuied A, McGarvey CP, Harb Z, Smith CC, et al. Diagnosis of glenoid labral tears using 3-test MRI vs 3-tesla MRA: a systematic review and meta-analysis. Arch Orthop Trauma Surg. 2018;138(5):699–709. https://doi.org/10.1007/s00402-018-2894-0.
22. Rerko MA, Pan X, Donaldson C, et al. Comparison of various imaging techniques to quantify glenoid bone loss in shoulder instability. J Shoulder Elbow Surg. 2013;22(4):528–34. https://doi.org/10.1016/j.jse.2012.05.034.
23. Acid S, Le Corroller T, Aswad R, et al. Preoperative imaging of anterior shoulder instability: diagnostic effectiveness of MDCT arthrography and comparison with MR arthrography and arthroscopy. AJR Am J Roentgenol. 2012;198:661–661. https://doi.org/10.2214/AJR.11.7251.
24. Lecouvet FE, Simoni P, Koutaïssoff S, et al. Multidetector spiral CT arthrography of the shoulder: clinical applications and limits, with MR arthrography and arthroscopic correlations. Eur J Radiol. 2008;68:120–36. https://doi.org/10.1016/j.ejrad.2008.02.025.
25. Green CK, Scanaliato JP, Sandler AB, et al. Risk factors for glenoid bone loss in the setting of posterior glenohumeral instability. Orthop J Sports Med. 2023;11(10):23259671231202300. https://doi.org/10.1177/23259671231202301.
26. Hines A, Cook JB, Shaha JS, et al. Glenoid bone loss in posterior shoulder instability: prevalence and outcomes in arthroscopic treatment. Am J Sports Med. 2018;46(5):1053–7. https://doi.org/10.1177/0363546517750628.
27.• Bedrin MD, Owens BD, Dickens JF. Prospective evaluation of posterior glenoid bone loss after first-time and recurrent posterior glenohumeral instability events. Am J Sports Med. 2022;50(11):3028–35. https://doi.org/10.1177/03635465221115828. **This recent study demonstrates an association between glenoid bone loss and posterior glenohumeral instability events and increased degree of bone loss with recurrent instability events.**
28. Arner JW, Ruzbarsky JJ, Midtgaard K, et al. Defining critical glenoid bone loss in posterior shoulder capsulolabral repair. Am J Sports Med. 2021;49(8):2013–9. https://doi.org/10.1177/0363546521016804.
29. Wolfe JA, Elsenbeck M, Nappo K, et al. Effect of posterior glenoid bone loss and retroversion on arthroscopic posterior glenohumeral stabilization. Am J Sports Med. 2020;48(11):2621–7. https://doi.org/10.1177/0363546520946101.
30. Lee RK, Griffith JF, Tong MM, et al. Glenoid bone loss: assessment with MR imaging. Radiology. 2013;267(2):496–502. https://doi.org/10.1148/radiol.12121681.
31. Bois AJ, Fening SD, Polster J, Jones MH, Miniaci A. Quantifying glenoid bone loss in anterior shoulder instability: reliability and accuracy of 2-dimensional and 3-dimensional computed tomography measurement techniques. Am J Sports Med. 2012;40(11):2569–77. https://doi.org/10.1177/0363546512458247.
32. Min KS, Sy JW, Mannino BJ. Area measurement percentile of 3-dimensional computed tomography has the highest interobserver reliability when measuring anterior glenoid bone loss. Arthroscopy. 2023;39(6):1394–402. https://doi.org/10.1016/j.arthro.2022.12.035.
33. Sgroi M, Huzurudin H, Ludwig M, Zippelius T, Reichel H, Kappe T. MRI allows accurate measurement of glenoid bone loss. Clin Orthop Relat Res. 2022;480(9):1731–42. https://doi.org/10.1097/CORR.0000000000002215.
34. Weber AE, Bolia IK, Horn A, Villacis D, Omid R, Tibone JE, et al. Glenoid bone loss in shoulder instability: superiority of three-dimensional computed tomography over two-dimensional magnetic resonance imaging using established methodology. Clin Orthop Surg. 2021;13(2):223–8. https://doi.org/10.4055/cios20097.
35. Breighner RE, Endo Y, Konin GP, Gulotta LV, Kof MF, Potter HG. Technical developments: zero echo time imaging of the shoulder: enhanced osseous detail by using MR imaging. Radiology. 2018;286(3):960–6. https://doi.org/10.1148/radiol.2017170906.
36. de Mello RAF, Ma YJ, Ashir A, Jerban S, Hoenecke H, Carl M, et al. Three-dimensional zero echo time magnetic resonance imaging versus 3-dimensional computed tomography for glenoid bone assessment. Arthroscopy. 2020;36(9):2391–400. https://doi.org/10.1016/j.arthro.2020.05.042.
37. Aydingoz U, Yidiz AE, Ergen FB. Zero echo time musculoskeletal MRI: technique, optimization, applications, and pitfalls. Radiographics. 2022;42(5):1398–414. https://doi.org/10.1148/rg.220029.
38. Saupe N, White LM, Bleakney R, Schweitzer ME, Recht MP, Jost B, Zanetti M. Acute traumatic posterior shoulder dislocation: MR findings. Radiology. 2008;248(1):185–93. https://doi.org/10.1148/radiol.2481071003.
39. Blum A, Coudane H, Mole D. Glenohumeral instabilities. Eur Radiol. 2000;10:63–80. https://doi.org/10.1007/s003300050008.
40. Harper KW, Helms CA, Haystead CM, et al. Glenoid dysplasia: incidence and association with posterior labral tears as evaluated on MRI. Am J Roentgenol. 2005;184:984–8. https://doi.org/10.2214/ajr.184.3.01840984.
41. Weishaupt D, Zanetti M, Nyffeler RW, Gerber C, Hodler J. Posterior glenoid rim deficiency in recurrent (atraumatic) posterior shoulder instability. Skeletal Radiol. 2000;29:204–10. https://doi.org/10.1007/s002560050594.
42. Currarino G, Sheffield D, Twickler D. Congenital glenoid dysplasia. Pediatr Radiol. 1998;28:30–7. https://doi.org/10.1007/s002470050287.
43. Albano D, Messina C, Sconenza LM. Posterior shoulder instability: what to look for. Magn Reson Imaging Clin N Am. 2020;28(02):211–21. https://doi.org/10.1016/j.mric.2019.12.005.
44. van de Brunt F, Pearl ML, Lee EK, et al. Glenoid version by CT scan: an analysis of clinical measurement error and introduction of a protocol to reduce variability. Skeletal Radiol. 2015;44:1627–35. https://doi.org/10.1007/s00256-015-2207-4.
45. Galvin JW, Parada SA, Li X, Eichinger JK. Critical findings on magnetic resonance arthrograms in posterior shoulder instability compared with an age-matched controlled cohort. Am J Sports Med. 2016;44(12):3222–9. https://doi.org/10.1177/0363546516660076.
46. Imhoff FB, Camenzind RS, Obopilwe E, et al. Glenoid retroversion is an important factor for humeral head centration and the biomechanics of posterior shoulder stability. Knee Surg Sports Traumatol Arthrosc. 2019;27:3952–61. https://doi.org/10.1007/s00167-019-05573-5.
47. Privitera DM, Siegel EJ, Miller LR, et al. Glenoid version and its relationship to glenohumeral instability and labral tears. J Shoulder Elbow Surg. 2016;25(7):1056–63. https://doi.org/10.1016/j.jse.2015.11.013.
48. Friedman RJ, Hawthorne KB, Genez BM. The use of computerized tomography in the measurement of glenoid version. J Bone Joint Surg Am. 1992;74:1032–7.
49. Harish S, Nagar A, Moro J, et al. Imaging findings in posterior instability of the shoulder. Skeletal Radiol. 2008;37(8):693–707. https://doi.org/10.1007/s00256-008-0487-7.

50. Robinson CM, Seah M, Akhtar MA. The epidemiology, risk of recurrence, and functional outcome after an acute traumatic posterior dislocation of the shoulder. J Bone Joint Surg Am. 2011;93(17):1605–13. https://doi.org/10.2106/JBJS.J.00973.
51. Moroder P, Tauber M, Hoffelner T, Auffarth A, et al. Reliability of a new standardized measurement technique for reverse Hill-Sachs lesions in posterior shoulder dislocations. Arthroscopy. 2013;29(3):478–84. https://doi.org/10.1016/j.arthro.2012.10.016.
52. Moroder P, Tauber M, Scheibel M, et al. Defect characteristics of reverse Hill-Sachs lesions. Am J Sports Med. 2016;44(3):708–14. https://doi.org/10.1177/0363546515621286.
53. Brelin A, Dickens JF. Posterior shoulder instability. Sports Med Arthrosc Rev. 2017;25(3):136–43. https://doi.org/10.1097/JSA.0000000000000160.
54. Yu JS, Ashman CJ, Jones G. The POLPSA lesion: MR imaging findings with arthroscopic correlation in patients with posterior instability. Skeletal Radiol. 2002;31:396–9. https://doi.org/10.1007/s00256-002-0513-0.
55. Fitzpatrick D, Grubin J. Navigating the alphabet soup of labroligamentous pathology of the shoulder. Am J Orthop. 2016;45(2):58–60.
56. Kim SH, Ha KI, Yoo JC, et al. Kim's lesion: an incomplete and concealed avulsion of the posteroinferior labrum in posterior or multidirectional posteroinferior instability of the shoulder. Arthroscopy. 2004;20:712–20. https://doi.org/10.1016/j.arthro.2004.06.012.
57. Rebolledo BJ, Nwachukwu BU, Konin GP, Coleman SH, Potter HG, Warren RF. Posterior humeral avulsion of the glenohumeral ligament and associated injuries: assessment using magnetic resonance imaging. Am J Sports Med. 2015;43(12):2913–7. https://doi.org/10.1177/0363546515606427.
58. Taljanovic MS, Nisbert JK, Hunter TB, et al. Humeral avulsion of the inferior glenohumeral ligament in college female volleyball players caused by repetitive microtrauma. Am J Sports Med. 2011;39(5):1067–76. https://doi.org/10.1177/0363546510391155.
59. Magee T. Prevalence of HAGL lesions and associated abnormalities on shoulder MR examination. Skeletal Radiol. 2014;43:307–13. https://doi.org/10.1007/s00256-013-1778-1.
60. George MS, Khazzam M, Kuhn JE. Humeral avulsion of glenohumeral ligaments. J Am Acad Orthop Surg. 2011;19:127–33. https://doi.org/10.5435/00124635-201103000-00001.
61.• Derrick M, Knapik DM, Patel HH, Smith MV et al. Posterior humeral avulsion of the glenohumeral ligament: a critical analysis review. JBJS Reviews. 2022;10(8) https://doi.org/10.2106/JBJS.RVW.22.00072. **A well written review and discussion of the biomechanical explanation for the PHAGL lesion, associated physical exam and imaging findings and treatment strategies.**
62. Bui-Mansfield LT, Taylor DC, Uhorchak JM, et al. Humeral avulsions of the glenohumeral ligament: imaging features and a review of the literature. AJR. 2002;179(3):649–55. https://doi.org/10.2214/ajr.179.3.1790649.
63. Bennett GE. Shoulder and elbow lesions of the professional baseball pitcher. JAMA. 1941;117(7):510–4.
64. Lombardo SJ, Jobe FW, Kerlan RK, Carter VS, Shields CL. Posterior shoulder lesions in throwing athletes. Am J Sports Med. 1977;5(3):106–10. https://doi.org/10.1177/036354657700500302.
65. Karich J, Kazam JK, et al. Bennett lesions in overhead athletes and associated shoulder abnormalities on MRI. Skeletal Radiol. 2019;48:1233–40. https://doi.org/10.1007/s00256-019-03176-2.
66. Ferrari JD, Ferrari DA, Coumas J, Pappas AM. Posterior ossification of the shoulder: the Bennett lesion- etiology, diagnosis, and treatment. Am J Sports Med. 1994;22:171–5. https://doi.org/10.1177/036354659402200204.